Korean J. Chem. Eng., 36(1), 126-135 (2019)
DOI: 10.1007/s11814-018-0139-0

pISSN: 0256-1115
eISSN: 1975-7220

Nickel nanoparticles-doped rhodamine grafted carbon nanofibers as colorimetric probe: Naked eye detection and highly sensitive measurement of aqueous Cr^{3+} and Pb^{2+}

Dinesh Kumar*,† and Neetu Talreja**

*School of Chemical Sciences, Central University of Gujrat, Gandhinagar 382030, India
**Center for Environmental Science and Engineering, Indian Institute of Technology Kanpur, Kanpur 208016, India
(*Received 13 April 2018 • accepted 5 August 2018*)

Abstract−Nickel nanoparticle (NiNPs)-doped carbon nanofiber (CNF) grafted with Rhodamine-B (RhB) dye (Ni-CNF-RhB), was prepared and utilized as a colorimetric probe for detection and measurements of chromium (Cr^{3+}) and lead (Pb^{2+}) metal ions in aqueous systems. An intense pink solution was obtained within 30 s on the exposure of the colorless Ni-CNF-RhB probe to the metal ions (Cr^{3+} and Pb^{2+}) solution. Briefly, the NiNPs-doped carbon beads were synthesized and applied as a substrate to grow CNFs by chemical vapor deposition. The Ni-CNF-RhB colorimetric probe exhibited fast response and selective determination towards Cr^{3+} and Pb^{2+} over the 0.1-10 ppm concentration range of their respective solution pH. The developed probe also showed the pH-dependent colorimetric response, thereby, selectivity determination of the metal ions. The detection limits of the colorimetric probe against Cr^{3+} and Pb^{2+} are 203 and 132 nM, respectively. The binding ability of the RhB-dye was augmented by CNF and NiNPs, while the carbon beads provided support to CNF to help probe in detection application and its re-usability. The method to prepare the colorimetric probe is simple, novel, selective, and the probe can be efficiently used for the fast detection (naked eye) and measurements of toxic metal ions in aqueous systems.

Keywords: Carbon Nanofibers, Rhodamine Dye, Colorimetric, Sensor, Toxic Metals

INTRODUCTION

The contamination of groundwater with toxic metal ions is one of the major environmental concerns. Metal ions such as chromium, arsenic, lead, mercury, and cadmium are extremely harmful to living organisms and are highly toxic even in parts per million (ppm) or sub-ppm concentrations in water [1]. Moreover, these metal ions initially present at trace levels [2], being non-biodegradable, these metal ions gradually accumulate in natural water bodies, and can eventually harm the living organisms through bioaccumulation. The monitoring and early detection of these metal ions in aqueous systems is, therefore, vital because of their ecologically hazardous effects. Various methods have been used for detecting and measuring them in water, such as atomic absorption spectroscopy, inductively coupled plasma emission spectroscopy, and high-performance liquid chromatography [3]. Although these methods are accurate, they are expensive, time-consuming and involve complex procedures. Further, these methods are commonly suited for analyses in laboratories and require adept hands. However, none of the probes developed so far has completely fulfilled all the criteria. Therefore, there is a strong need for developing a simple, fast, portable and cost-effective probe for the detection and measurements of toxic metal ions in water.

In view of these limitations, various research groups have developed fluorescent and colorimetric probes that can selectively respond to the presence of metal ions in water [4]. Such probes have been developed using different fluorescent agents, such as organic luminescent dye-metal complexes [5], carbon dots [6], organic chromophore compounds [7,8], polymeric fibers [9], and, proteins [10]. Metal nanoparticles (MNPs)-based fluorescent and colorimetric probes, such as AgNPs [11] and AuNPs [12,13] have also been used for chemical and biological detection. Nonetheless, their response time is relatively higher with the use of expensive metal NPs.

The colorimetric probes are effective, fast, and simple to use for detecting heavy metal ions in water and recommended for field use. Indeed, such probes have been widely used for determining different cations and anions in water [14,15]. The challenge in developing an effective colorimetric probe for detecting metal ions is to identify an appropriate combination of inexpensive metal and dye with strong binding, capable of producing sufficiently intense color for naked-eye detection and is also definitively selective and sensitive.

Rhodamine (RhB) dye is extensively used as a colorimetric and fluorescence labeling reagent because of its excellent spectroscopic properties, including long absorption and emission wavelengths, large absorption coefficient, and high fluorescence quantum yield [16]. The mechanism of sensing metal ions by the RhB-based devices is structural change between the different RhB derivatives. For example, the spirolactam form of RhB is colorless and non-fluorescent, whereas its metal-induced open ring amide form has strong absorption within the visible range, displaying strong fluorescence emission and color [16-18]. However, RhB cannot be directly used for sensing applications since it is itself a colored dye. Upon directly

†To whom correspondence should be addressed.
E-mail: dinesh.kumar@cug.ac.in

contacting even in fresh water without metal ions, it dissolves quickly, producing intense pink color. Therefore, a suitable support is required to fortify the dye in water, which can also facilitate controlled leaching in the metal-laden water, producing color.

Carbon-based nanomaterials are the next generation of materials for several environmental applications [19]. The significance of these materials is in their distinct physicochemical characteristics, such as large surface area and amenability to surface functionalization [20-22]. In the present context, carbon nanotubes (CNTs) have been used for analytical applications. The organic dye-modified CNTs were developed by Ahmad et al. [23], for sensing metal ions, with enhanced color intensity. Similarly, with an elaborate choice available, nanomaterials have also been used for the detection of heavy metal ions, with high selectivity and fast response, using electrochemical techniques [24]. Although potentially attractive materials as sensors for metal ions, such nanomaterials must be effectively attached to a suitable micron-sized substrate to be used in practical applications.

Recently, the micron-sized porous carbon beads [25] and carbon beads decorated with carbon nanofibers (CNFs) by the catalytic chemical vapor deposition (CVD) technique [26-28] were developed as efficient materials for environmental remediation applications. These CNFs-decorated Ni-carbon beads (Ni-CNFs) are capable of chemical modification of CNFs surfaces. NiNPs on the tip of the fibers has been utilized as a fluorescence quencher. In the present study, nickel catalyzed CNFs grown on carbon beads (~0.5 mm) were grafted with RhB and used as an efficient colorimetric probe for fast detection, and measurement of different toxic metal ions, namely, Cr^{3+} and Pb^{2+} in water. The physicochemical properties of the prepared materials were characterized, and the effects of pH and metal ion concentrations (0.1-10 ppm) on the response of the prepared Ni-CNF-RhB probe were determined.

The novelty of the present study is as follows. (1) CNF increase the binding ability of the RhB, thereby, the formation of efficient probes, (2) the presence of Ni on the surface of CNF has also enhanced the binding ability of the RhB, and (3) the carbon beads provide support of the CNF, which is beneficial for the probe during application and its re-usability. Therefore, the present work lies in the facile and fast naked eye determination of Cr^{3+} and Pb^{2+} ions at very low concentration without the use of any sophisticated instrument.

MATERIALS AND METHOD

1. Chemicals

Phenol, formaldehyde, triethylamine (TEA), hexamethylenetetramine (HMTA), polyvinyl alcohol (PVA), RhB and ethylenediamine (EDA), $Cr(NO_3)_3$, $Pb(NO_3)_2$ salts were used as received. All reagents were of high purity grade, and all samples were prepared in Milli-Q water.

2. Synthesis of Activated Carbon Beads

Phenolic precursor beads were prepared as per the procedure described in the previous study [22]. Briefly, beads were synthesizing a suspension polymerization. A mixture of phenol (50 g), formaldehyde (63 mL) and TEA (1.5 mL), used as a monomer, solvent, and catalyst, respectively, was stirred for 8 h in a round bottom flask at room temperature (~30 °C). Next, 200 mL of deionized water (DI) was added to the flask. Hexamine (3.5 g), used as the cross-linking agent, was added to the reaction mixture. The solution was heated at the rate of 3 °C per min until the temperature of the mixture was 100 °C. After 15 min, 3 g of PVA was added as a suspension stabilizing agent in the reaction mixture. A gel began to form approximately 30 min after adding PVA. At the incipience of the gel formation, Nickel nitrate (15% w/w of phenol) was added to the mixture. The beads (~0.8 mm), produced approximately after 3 h, were washed repeatedly with acetone, water, and methanol, and then dried at room temperature.

The dried Ni-doped phenolic beads (Ni-PhBs) were kept in a tubular horizontal reactor (30 mm diameter and 1,000 mm length), installed in an electrical furnace, for carbonization and activation. Carbonization was performed at 900 °C for 1 h under an inert nitrogen atmosphere, whereas activation was performed using steam as the activating agent at the same temperature for 1 h. After activation, the Ni-doped porous carbon beads (Ni-PhB-A) were produced. Approximately 40% of weight-loss was observed in the beads during carbonization/activation, and the average particle diameter decreased to ~0.5 mm.

3. The Growth of CNFs on Porous Carbon Beads

The carbon beads were subjected to reduction at 550 °C, using H_2 at 0.15 standard liters per min (slpm) flow rate. The Ni NPs, produced *in situ* after reduction, served as the CVD catalyst for growing CNFs on the beads. Acetylene was used as the carbon source. CVD was performed at 600 °C for 30 min, producing the Ni-doped carbon beads decorated with the CNFs (Ni-CNF-PhB).

4. Grafting of Ni-CNF-PhB with RhB

Grafting was performed on ~1 g of Ni-CNF-PhB, using a mixture of 0.5 g RhB, 50 mL ethanol and 10 mL EDA in a 100 mL flask. The reaction mixture was stirred for 24 h. After washing, the prepared materials (Ni-CNF-RhB) were stored at room temperature and directly tested as the probes for the detection of metals in water.

5. Preparation of CNF-probes Using Different Metals

CNF-probes were also prepared using Zn and Fe metal NPs as the CVD catalyst for the comparison purposes. First, carbon beads were prepared for the *in situ* doped polymeric beads, based on the same procedure that was earlier described for the synthesis of Ni-PhBs. CNFs were grown on the beads by CVD, using Zn or Fe as the catalyst, and the prepared Zn- and Fe-CNF-PhB were grafted with RhB and tested as the probe. The synthesis conditions for growing the CNFs using Fe and Ni, including impregnation, calcination, reduction, and CVD are described in the studies of Talreja et al. [26,27].

6. Absorbance Measurement

The absorbance of the metal salt solutions (Cr^{3+} and Pb^{2+}) was measured over 400-800 nm wavelength, using a UV-Vis spectrophotometer (Carry 100, Varian, USA). The tests were performed on ~0.01 g of the prepared Ni-CNF-RhB beads mixed in 10 mL metal ion solutions. All tests were performed in triplicate to check the reproducibility.

Fig. 1 shows the UV-Vis spectra and photograph of Cr^{3+} and Pb^{2+} ions in aqueous solution at pH ~4.5 and 3.5, respectively. The spectra are shown for the measurements performed for 10 ppm metal solutions. In each case, maximum peak intensity was observed

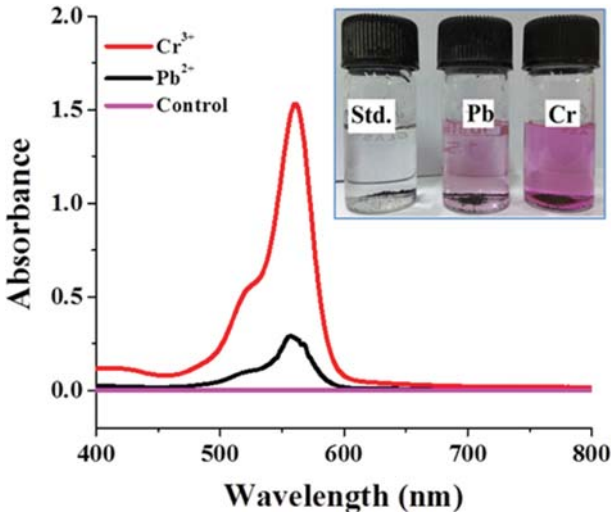

Fig. 1. Absorbance vs. wavelength plots for different metals at solution pH (inset Fig. shows the visible changes after exposure to metal ions).

at 553 nm for all metals, and therefore, all measurements in this study were performed at the 553 nm. The minimum absorbance was 0.0346, which corresponded to 0.1 ppm. Maximum variation in the reported absorbance in this study is less than ±10%.

The representative photograph (inset of Fig. 1) of the metal solutions exposed to the prepared probe materials, along with the control. The DI water (without any metal ions) mixed with Ni-CNF-RhB was used as the control, and it was colorless. The metal solutions, however, turned pink when the beads (probe) were added, and the color intensity varied depending on the metal concentrations. The RhB derivatives with a closed ring structure are non-fluorescent, whereas its open ring structure known as spirolactam gives rise to an intense color. Only the Pb^{2+} and Cr^{3+} ions exhibited color at solution pH, as is later discussed.

Calibration plots with different concentration ranges (0.1, 0.5, 1, 5, 10 ppm) were used to determine the limit of detection and limit of quantification of the prepared Ni-CNF-RhB probes. The detection limit and quantitation limit were calculated by using a linear regression line.

7. Fluorescence Spectrophotometry Analysis

The fluorescence intensity of the prepared Ni-CNF-RhB probe was determined by using a fluorescence spectrophotometer (Carry Eclipse, Varian, USA). The spectra were recorded at after 1 min exposure of probe with Cr^{3+} and Pb^{2+} at different concentration (0.1, 0.5, 1, 5 and 10 ppm) ranges by using ~0.01 g Ni-CNF-RhB probe in a 10 mL metal ion solution.

8. Regeneration of the Probe

The regeneration of Ni-CNF-RhB probe was tested for Cr^{3+} metal ions. The probe was regenerated at 400 °C in an inert atmo-

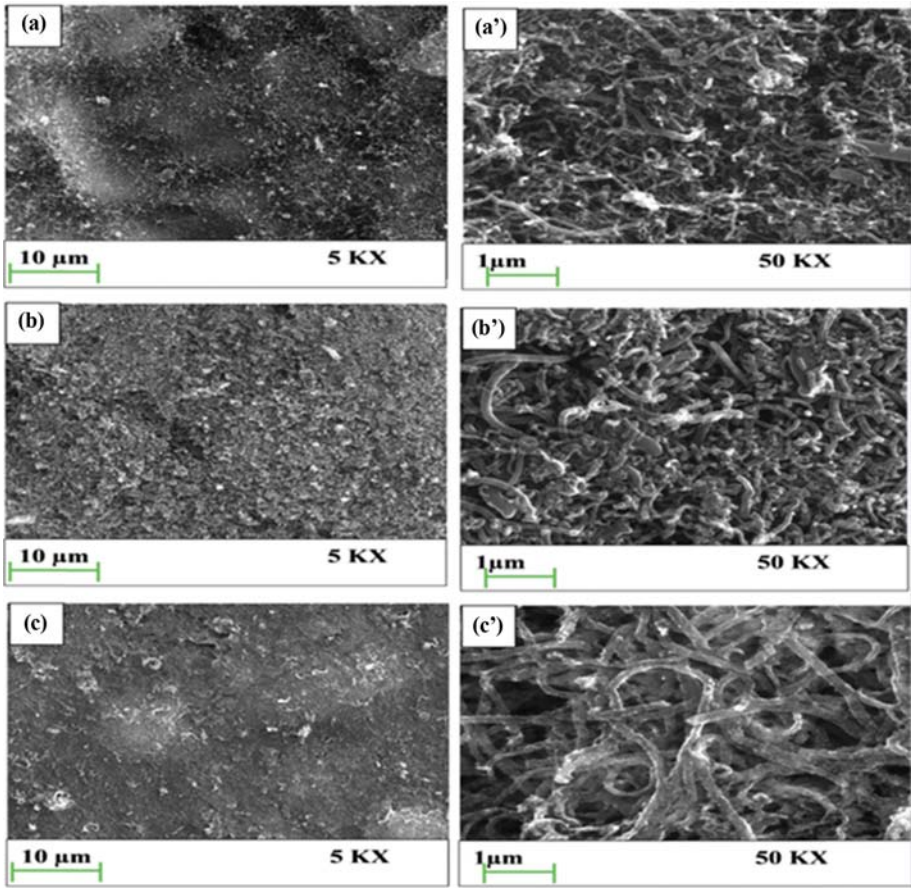

Fig. 2. SEM images of (a)-(a′) Ni-CNF-PhB, (b)-(b′) Ni-CNF-RhB, and (c)-(c′) Ni-CNF-RhB after exposure to metal solution.

sphere of N_2 to remove attached metal ions. After regeneration, the Ni-CNF-RhB probe was further tagged with the RhB-dye, as described procedure discussed earlier in the text.

SURFACE CHARACTERIZATION

The surface morphology of the prepared samples was observed using a field emission scanning electron microscope (FESEM, MIRA3 TESCAN) and Tecnai G 2 20 (FEI) S-Twin transmission electron microscope. The metal content in the samples was determined by EDX analysis (Oxford, Inca, Germany).

Various functional groups on the surface of the prepared samples were determined using FTIR (Tensor 27, Bruker, Germany) over the wavenumber range of 400-4,000 cm^{-1}, using an attenuated total reflectance with the germanium crystal. Throughout the analysis, the sample chamber of the instrument was purged with N_2 gas to reduce the effect of atmospheric carbon dioxide and moisture. The background spectrum was recorded before the measurements. The resolution was set to 4 cm^{-1}, and a total of 100 scans was collected for each sample.

1. SEM Analysis

Fig. 2(a) and (a′) show low and high magnification SEM images of Ni-CNF-PhB. Dense and thin fibers were grown on the surface of the beads. The metal NPs can be observed at the tips of the nanofibers in the high magnification image. Fig. 2(b) and (b′) show the SEM images of Ni-CNF-RhB. The surface morphology completely changed after grafting. Low magnification images show whitish precipitate on the surface of the material, indicating that the CNFs is covered with RhB during grafting. Additionally, the fibers became thick after grafting (Fig. 2(b′)). Fig. 2(c) and (c′) show the SEM images of the probe material (Ni-CNF-RhB) upon exposure to the Cr test solution. The fibrous texture disappeared completely because of the adherence of the metal ions onto the surface of the fibers, commensurate with the morphology of the material observed in the SEM images of the materials exposed to other metal ions in this study.

2. Energy Dispersive x-ray Analysis

Fig. 3(a)-(c) shows the EDX analysis of the prepared materials before and after using them for the detection of Cr^{3+} and Pb^{2+} ions in water and elemental mapping of the Ni-CNF-RhB. The EDX spectra (point analysis) of the Ni-CNF-RhB beads validated the presence of the Ni in the samples, along with C and O. The EDX spectra of the Ni-CNF-RhB beads, exposed to the Cr^{3+} and Pb^{2+} solutions, confirmed the presence of the respective metal in the samples. The EDX spectra of the samples exposed to other metal solutions also corroborated the presence of respective metal in the solutions. (they are not included here for brevity). Fig. 3(d) shows the elemental mapping of the Ni-CNF-RhB sample. The elemental

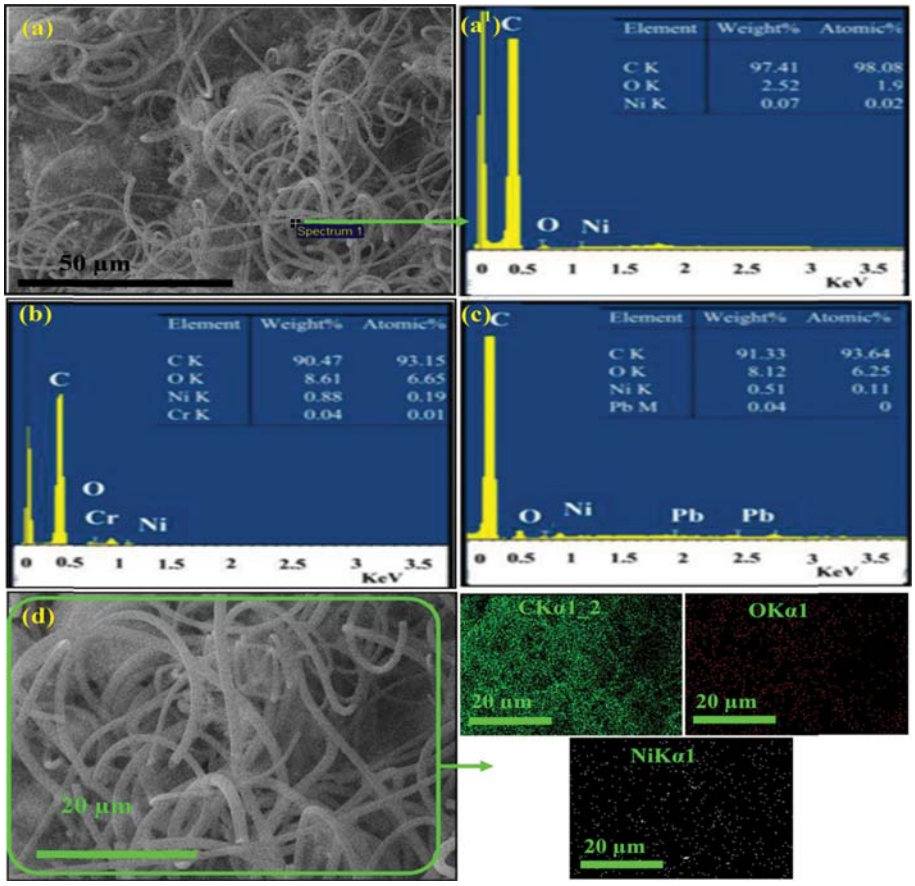

Fig. 3. EDX spectra of Ni-CNF-RhB (before and after metal detection) (a)-(a′). Ni-CNF-RhB point analysis (b). Ni-CNF-RhB after adsorption of Cr^{3+} (c). Ni-CNF-RhB after adsorption of Pb^{2+}, and (d) elemental mapping of Ni-CNF-RhB.

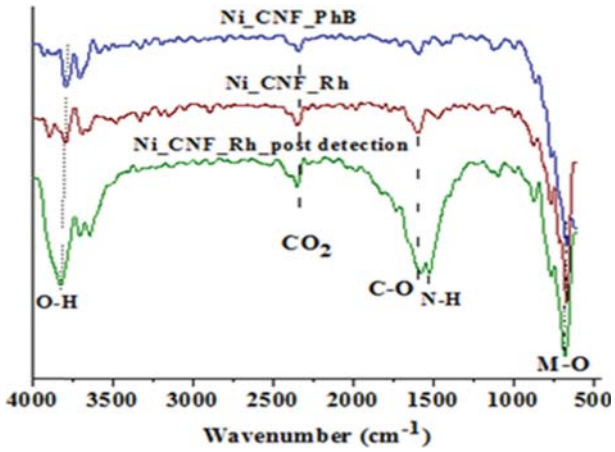

Fig. 4. FTIR analysis of different material Ni-CNF-PhB, and Ni-CNF-RhB (before and after exposure to Cr^{3+} solution).

mapping confirms the small metal nanoparticles are Ni and metal nanoparticles uniformly distributed within the Ni-CNF-RhB sample.

3. FTIR Analysis

Fig. 4 shows the FTIR spectra of Ni-CNF-PhB, and Ni-CNF-RhB (before and after exposure to Cr^{3+} ions). Common peaks were observed at 2,350 and 3,600-3,700 cm^{-1} in all samples, corresponding to the carbon dioxide and O-H groups of hydroxyls, respectively. The grafting of Ni-CNF-PhB with RhB increased the peak intensity of the C-O group, which is attributed to the carbonyl group of the RhB molecule. The existence of the band at 1,584 cm^{-1} indicated the deposition of RhB [29]. The spectra of Ni-CNF-RhB exposed to Cr metal ions showed significant increase in the stretching of C-O, N-H and M-O, OH groups (1,603, 1,522 and 650, 3,798 cm^{-1} respectively), indicating that these groups participated in the bonding with the metal ions, and confirming the ring opening mechanism for RhB in the prepared material, the results of which are in good agreement with previous report [30]. The ring opening occurred by the binding event involving both the carbonyl O and the imino N atoms, forming a stable 5-membered cyclic complex that opened the ring of RhB derivative [16]. Similar changes in the stretching were observed in the FTIR spectra recorded for the Ni-CNF-RhB samples exposed to the other metal solutions.

RESULTS AND DISCUSSION

1. Effect of Metal Concentrations

The effects of metal concentrations on the response of the Ni-CNF-RhB probe were determined over the concentration ranges (0.1-10 ppm). Fig. 5(a) and (b) show the effects of concentration on the detection of Cr^{3+} and Pb^{2+} metal ions, which were detectable at the solution pH over the entire concentration range. The absorbance increased with increasing concentrations of both metal ions, whereas, above 10 ppm, color, diminish, and on further increasing the concentration, no color was visible. The color of Pb^{2+} and Cr^{3+} solutions appeared within 30 s after adding Ni-CNF-RhB, while no color was visible or detected in the other metal ion solutions. The Cr^{3+} solution exhibited faster response and higher absorbance intensity than the Pb^{2+} solution. Also, the absorbance continuously in-

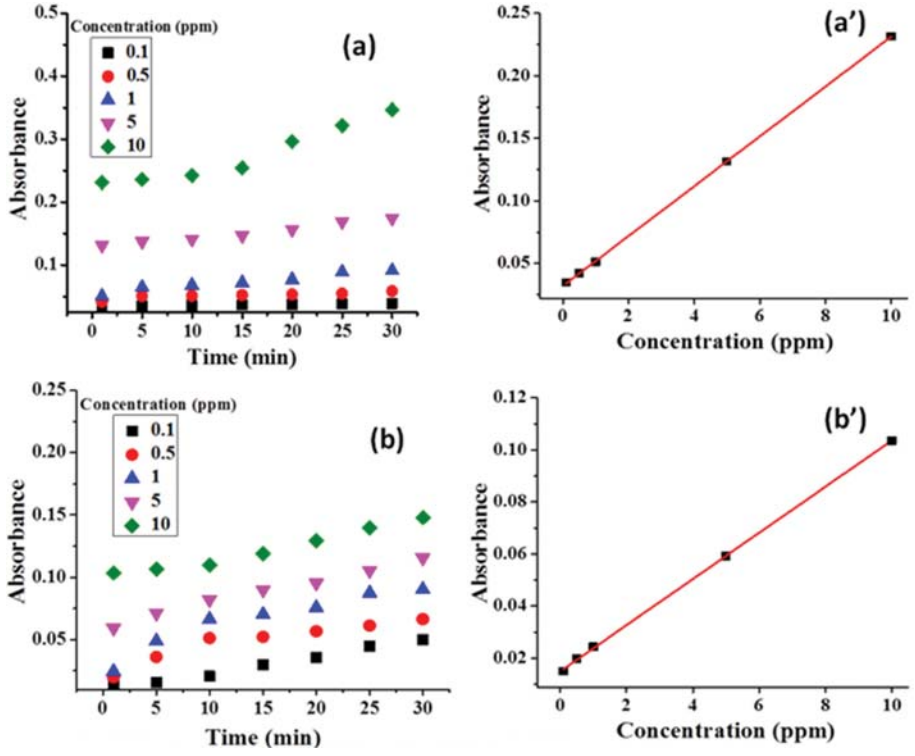

Fig. 5. The absorbance of Ni-CNF-RhB probe upon exposure to different concentration (0.1-10 ppm) ranges of Cr^{3+} and Pb^{2+}, (a) and (a′) temporal variation in the absorbance and calibration plot of Cr^{3+}, (b) and (b′) temporal variation in the absorbance and calibration plot of Pb^{2+}.

Table 1. Different probe used for the determination of Cr^{3+} and Pb^{2+} metal ions

Probe	Metal ion	Response time (min)	LOD (nM)	References
Ni-CNF-RhB	Cr^{3+}	0.5	203 nM	Present study
Ni-CNF-RhB	Pb^{2+}	0.5	132 nM	Present study
Schiff base ligands (AP1 & AP2)	Cr^{3+}	10	960 and 1210	Kumawat et al. [31]
Glutathione-stabilized gold nanoclusters	Cr^{3+}	30	49	Zhang et al. [32]
CdS quantum dots	Cr^{3+}	-	23	Abolhasani et al. [33]
Citrate capped gold nanoparticles	Cr^{3+}	5	101	Rajeshwari et al. [34]
Gold nanoparticles	Cr^{3+}	20	16	Wang et al. [35]
Gold nanoparticle-loaded polymer brushes	Pb^{2+}	45	0.25	Ferhan et al. [36]
Gold nanoparticle probes	Pb^{2+}	20	500	Wei et al. [37]
Gold nanoparticles	Pb^{2+}	0.33	25	Ding et al. [38]
G-quadruplex DNAzyme (PS2.M)	Pb^{2+}	4	0.97	Li et al. [39]
Gold nanoparticles (Au NPs) probes	Pb^{2+}	15	0.92	Kuang et al. [40]

creased with increasing the concentration. The formation of color on exposure to metal ions was due to the delactonization process, which convert spirocyclic (or colorless) form of RhB of its ring-opened form. The fast response in the Cr solution is attributed to the vacant d-orbital of the metal, which acts as an acceptor orbital and utilizes the electron transfer from the RhB donor molecule. Similarly, Pb^{2+} atoms have vacant p-orbitals which can accept an electron and enhance color. The amount of chelation-enhanced color intensity depends on the ligand nature and interacting metal ions. The properties of metal ions such as magnetic behavior and vacant orbital play a significant role in the formation of color intensity and are the reasons for the colors of Cr^{3+} and Pb^{2+} metal ions. Metal ions interacted with the oxygen and nitrogen present in RhB ring and formed a stable complex, and the electron density shifted toward the metal binding site and exhibited color [31]. The data indicate that the prepared probe showed a definitive preference for the detection of Cr^{3+} and Pb^{2+} ions at low concentrations.

Fig. 5(a′) and (b′) shows the calibration plots of Cr^{3+} and Pb^{2+} metal ions. The calibration plots show the linear relationship in a concentration (0.1-10 ppm) ranges. The changes in the absorbance increased with increasing the concentration of both Cr^{3+} and Pb^{2+} metal ions. The regression coefficient was calculated to be 0.99 for both Cr^{3+} and Pb^{2+} metal ions. The detection limit of the prepared Ni-CNF-RhB probes against Cr^{3+} and Pb^{2+} metal ions was determined to be 203 and 132 nM, respectively, while the quantification limit was determined to be 615 and 400 nM, respectively. The signal to noise ratio (S/N) was calculated to be 3. The detection limit of the prepared Ni-CNF-RhB probes was comparable in the reported literature summarized in Table 1.

Table 1 data show that the prepared Ni-CNF-RhB probes were comparable to most of the studies based on the detection limit, while the response time of the preparation Ni-CNF-RhB probes was observed significantly higher compared with all studies reported in the literature [31-40]. Therefore, based on response time and detection limit, our probes show the potential ability for the detection of toxic metal ions from water.

2. Fluorescence Intensity Measurement

Fig. 6 shows the fluorescence sensing behavior of aqueous solutions of Cr^{3+} and Pb^{2+} metal ions. The fluorescence spectra show both metals Cr^{3+} and Pb^{2+} ions intense peak at approximately 580 nm. The fluorescence intensity increased with increasing the concentration of metal ions. As observed from the figure, the Cr^{3+} shows relatively higher fluorescence intensity than Pb^{2+} ions. The fluorescence data follow the similar trends with respect to the colorimetric sensing responses. The data also suggested that the prepared Ni-CNF-RhB is a colorimetric as a well fluorescent probe. The ring open structure of Cr^{3+} and Pb^{2+} is fluorescent and exhibiting maxima at 572 nm initially, at concentrations lower than 0.5

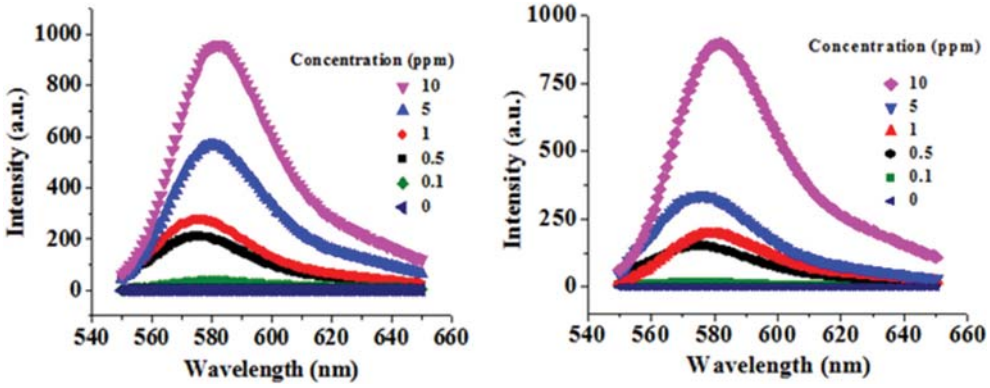

Fig. 6. Fluorescence intensity of metals ion at 0.1-10 ppm concentration: (a) Cr^{3+}, (b) Pb^{2+}.

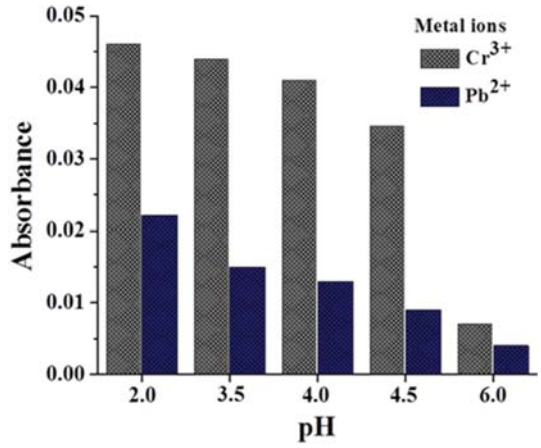

Fig. 7. Effect of pH on absorbance of Cr^{3+} and Pb^{2+} on Ni-CNF-RhB.

ppm. Upon increasing the concentration of Cr^{3+} and Pb^{2+}, giving rise to a new maximum at 585 nm, and the fluorescence intensity of this band rises with increasing concentrations of Cr^{3+} and Pb^{2+} metal ions. This suggests that metal ions shift the equilibrium between the amide and spirolactam forms of the RhB derivative due to the formation of "open" amide structure. Additionally, the development of color, which can be followed by UV/Vis spectroscopy or by the naked eye, is less intense than that observed in a solution of a Pb^{2+} metal ion with the same concentration of the sensory ions.

3. Effects of pH

Fig. 7 describes the effects of pH (2, 4, and 6) on the sensing response (changes in the absorbance) of the probe for the detection of metal ion solutions at 0.1 ppm concentration. Above pH ~6, metals precipitated in their respective solutions because of the formation of a hydroxide of respective metal ions. The color intensity increased with decreasing pH in both metal ions (Cr^{3+} and Pb^{2+}) solution. The Cr^{3+} solution exhibited pink color at solution pH (~4.5) within 30 s. However, the color disappeared on increasing the pH>~5 due to less viability of proton for RhB. In acidic metal solutions, the protonation of the carboxylic group of RhB induces the opening of the amide ring, which is faster compared to that in the normal solution pH [41]. Acidic pH gives pink color solution due to spirolactam ring opening, triggered by activation of a COOH group of RhB of the spirolactam ring by protonation due to acids.

4. Selectivity and Synthetic Water Analysis

The selectivity of the prepared Ni-CNF-RhB probes was determined by using different metals (Fe^{2+}, Co^{2+}, Mn^{2+}, Cu^{2+}, Hg^{2+}, As^{5+}, Ni^{2+}, and Cd^{2+}) including Cr^{3+} and Pb^{2+} ions at concentration 0.1 ppm. Fig. 8(a) shows the changes in the absorbance (sensing response) of Ni-CNF-RhB probes against different metal ions. It is clearly observed from the data Ni-CNF-RhB probes showed sensing response against Cr^{3+} and Pb^{2+} metal ions only due the paramagnetic characteristics of ions and vacant orbitals, while after exposure to other metal (Fe^{3+}, Co^{2+}, Mn^{2+}, Cu^{2+}, Hg^{2+}, As^{5+}, Ni^{2+}, and Cd^{2+}) ions, no changes in absorbance were observed because these metal ions do not have sufficient space for coordination with RhB ligand, and thereby, do not emit color [41]. Therefore, the prepared probes were selective against Cr^{3+} and Pb^{2+} metal ions.

Fig. 8(b) shows the synthetic water analysis study of the prepared Ni-CNF-RhB probes in the binary system of Cr^{3+} at 0.1 ppm, because of probes only sensitive against Cr metal ions, as earlier discussed in the manuscript. It was observed from the data, the changes in the absorbance were higher compared with Cr^{3+} and Pb^{2+} alone in the aqueous solution due to the changes in solution pH. The solution pH of Cr^{3+} was around ~4.5, and Pb^{2+} have ~3.5, while the solution pH of the binary system was measured ~4, at this pH change in the absorbance, was relatively higher in both metal Cr^{3+} and Pb^{2+} ions. The binary solution of Cr^{3+} and other metal cations such as Fe^{3+}, Mn^{2+}, Ni^{2+}, Cu^{2+}, and Hg^{2+} have no significant effect on absorbance due to the least chelation property of other metal ions.

5. The Response of Different Metal NPs-grown CNF Based Probes

As previously mentioned, Zn- and Fe-CNF-RhB were also prepared and tested as the probes for comparison purposes. Fig. 9 shows the absorbance measured in Cr^{3+} solutions at 10 ppm concentration within 15 min. Negligible absorbance (<0.01) was observed using the Fe NP-based probes. The Ni NPs-based probes showed significant absorbance at solution pH, which was considerably higher than that of the Zn NPs-based probes. The sensitivity of the Ni-CNF-RhB based probe is based on the stability of metal-RhB complexes and releases of RhB. The release of RhB from the probes depends upon the produces stable/unstable complexes. Being

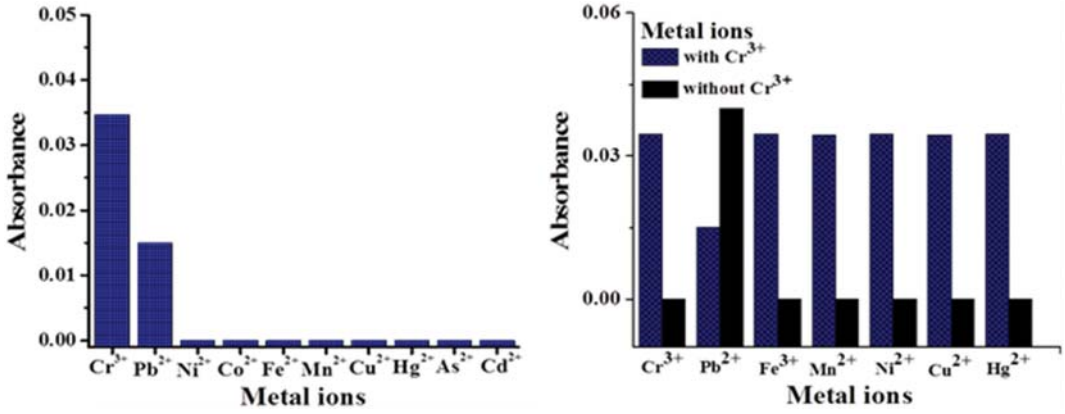

Fig. 8. Selectivity and interference of the Ni-CNF-RhB probe against metal ions, (a) selectivity (b) interference.

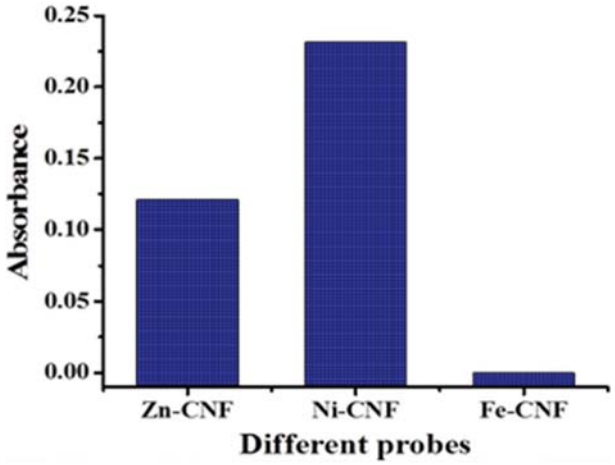

Fig. 9. Absorbance produced using different metal NP-prepared CNF probes during detections (Cr concentration=10 ppm).

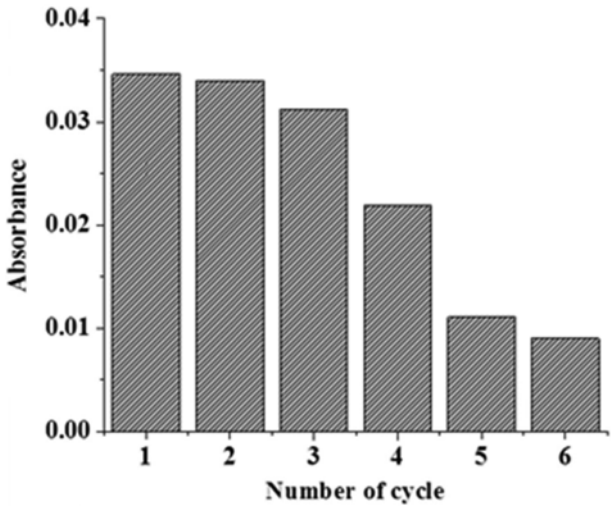

Fig. 11. Regeneration cycle of Ni-CNF-RhB based probe.

a cationic dye, RhB can interact with electron-donor species. The higher is the donation ability, the more stable is the formed metal-RhB complex. Moving along the column of transition metals in the periodic table the stability of the metal-RhB complexes increases because of increased effective nuclear charge of metal ions. Fe produces an unstable complex. The unstable complex of metal-RhB complexes indicates the relatively lesser amount of RhB bind with the metals, thereby, less sensitivity of the probes. On the other hand, Zn produces a stable complex and is unable to release RhB derivatives from the tips of the Zn-CNFs into the metal ion solution, thereby, slower release of RhB subsequently, relatively less sensitivity of the probes. The in-between placed Ni provides a controlled release of RhB for the sensing of metal ions [43,44], and therefore, Ni-CNF-RhB was used as the probe for the detection of toxic metal ions in this study.

6. Mechanism of Sensing

Based on the results discussed in the preceding sections, including the SEM and FTIR characterization data, a possible mechanism for the detection of the metal ions is illustrated in Fig. 10. The intensity of the product color depends on the ability of RhB to bind with the different metal ions, the binder support and pH of the solution. The RhB exhibits strong binding affinity to the metal ions possessing vacant orbital, which facilitates electron or charge transfer from the donor to the acceptor moiety. The metal ion induces the opening of spirolactam ring and is coordinated with the carbonyl oxygen atom and the amine nitrogen atom. When the nitrogen atom coordinates to metal ions, its electron donating ability towards RhB is reduced. The electron transfer from the N atom to the RhB system is precluded and the charge transfer from N atom to metal ions takes place, resulting in an intense pink color in the metal contaminated water solution [30]. On lowering the pH of the solution, the intensity of metal ions increases, due to the protonation of RhB at acidic pH, which facilitates the production of open chain structure and high-intensity color [31].

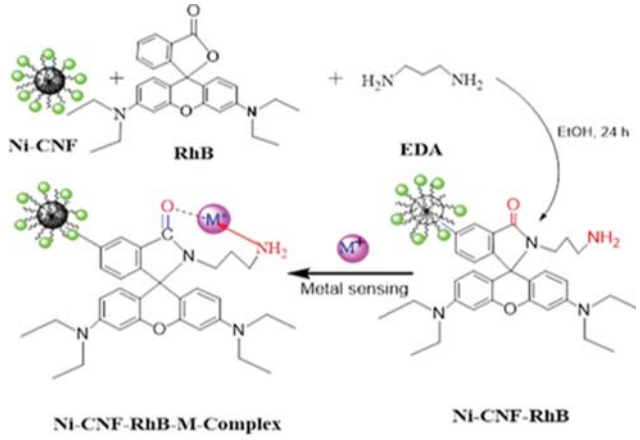

Fig. 10. Mechanism of metal ion detection by Ni-CNF-RhB.

7. Regeneration of the Ni-CNF-RhB Probes

The regeneration of the prepared Ni-CNF-RhB probe was determined and tested against Cr^{3+} ions at 0.1 ppm concentration. Fig. 11 shows the regeneration cycle of the prepared Ni-CNF-RhB probe. The data clearly indicated that the Ni-CNF-RhB probe was successfully used to the third cycle with no significant changes in the absorbance or sensing response. However, in the third cycle, approximately 30% decrease in the sensing response was observed, while after the fourth cycle a dramatic decrement in the responses was observed, which is due to the loss of the Ni-CNF during the regeneration process. Fig. 12(a) and (b) shows SEM images of CNF lower and higher magnification, respectively. As observed from the SEM images the diameter of Ni-CNF is reduced due to the regeneration. The band gap energy is directly related to the structure of nanomaterials, that depends on the CNF structure. After the third cycle, CNF starts degradation, subsequently, changes in the band gap energy, binding of RhB and sensing efficiency decreases. Therefore, data suggested that Ni-CNFs plays an efficient role in the binding of RhB-dye.

CONCLUSIONS

A novel colorimetric Ni-CNF-RhB-based sensor was success-

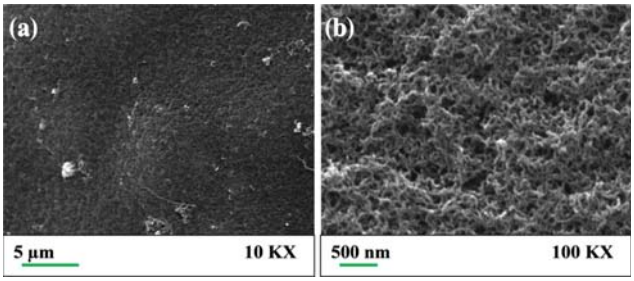

Fig. 12. SEM images showing degradation of Ni-CNF-RhB after 3rd cycle (a) at low magnification (b) at high magnification, respectively.

fully engineered and applied for the selective detection of Cr^{3+} and Pb^{2+} metal ions in water over the 0.1-10 ppm concentration range. The surface characterization data corroborated successful attachment (grafting) of Ni-CNF-PhB with the RhB dye. On contacting the probe with the metal solutions at the respective solution pH, the colorless solution turned pink in less than 30 s, with significant absorbance detected using UV-Vis spectrophotometry. The Ni NPs at the tips of the CNFs could effectively bind with RhB derivative, providing a fast response when the probe material was contacted with the toxic metals in water. Finally, the prepared Ni NPs grown CNFs, supported over the micron-sized carbon beads in this study, can be used as a robust, simple, portable, and efficient calorimetric probe for fast detection of common toxic metals in wastewater for field applications, and also, quantitative measurements of the metals, using a simply visible range-spectroscopy in the laboratory.

ACKNOWLEDGEMENTS

The authors acknowledge the Center for Environmental Science and Engineering at IIT Kanpur (India) for conducting the present study.

REFERENCES

1. I. Bontideana, A. Mortaria, S. Letha, N. L. Brownb, U. Karlsonc, M. M. Larsenc, J. Vangronsveldd, P. Corbisiere and E. Csoregi, *Environ. Pollut.*, **131**, 255 (2004).
2. F. Fu and Q. Wang, *J. Environ. Manage.*, **92**(3), 407 (2011).
3. P. Kuban, R. Guchardi and P. C. Hauser, *Trends Anal. Chem.*, **24**, 192 (2005).
4. H. N. Kim, W. X. Ren, J. S. Kim and J. Yoon, *Chem. Soc. Rev.*, **41**, 3210 (2012).
5. C. R. Lohani, J. M. Kim, S. Y. Chung, J. Yoon and K. H. Lee, *Analyst*, **135**, 2079 (2010).
6. A. Larki, *Spectrochim. Acta A.*, **173**, 1 (2017).
7. A. Halder and S. Bhattacharya, *Spectrochim. Acta A.*, **99**, 335 (2012).
8. Z. Tian, S. Cui, C. Zheng and S. Pu, *Spectrochim. Acta A.*, **173**, 75 (2017).
9. G. Li, L. Zhang, Z. Li and W. Zhang, *J. Hazard. Mater.*, **177**, 983 (2010).
10. V. H. C. Liao, M. T. Chien, Y. Y. Tseng and K. L. Ou, *Environ. Pollut.*, **142**, 17 (2006).
11. K. Farhadia, M. Forougha, R. Molaeia, S. Hajizadeha and A. Rafipour, *Sensor Actuat B-Chem.*, **161**, 880 (2012).
12. K. Saha, S. S. Agasti, C. Kim, X. Li and V. M. Rotello, *Chem. Rev.*, **112**, 2739 (2012).
13. H. Y. Chang, T. M. Hsiung, Y. F. Huang and C. C. Huang, *Environ. Sci. Technol.*, **45**, 1534 (2011).
14. H. E. Kaoutit, P. Estévez, S. Ibeas, F. García, F. Serna, F. B. Benabdelouahab and J. M. García, *Dyes Pigm.*, **96**, 414 (2103).
15. A. Liu, L. Yang, Z. Zhang, Z. Zhang and D. Xu, *Dyes Pigm.*, **99**, 472 (2013).
16. X. Zhang, Y. Shiraishi and T. Hirai, *Tetrahedron Lett.*, **48**, 5455 (2007).
17. O. Sunnapu, N. G. Kotla, B. Maddiboyina, S. Singaravadivel and G. Sivaraman, *RSC Adv.*, **6**, 656 (2016).
18. Z. Tang, X. L. Ding, Y. Liu, Z. M. Zhao and B. X. Zhao, *RSC Adv.*, **5**, 99664 (2015).
19. S. Xiao, M. Shen, R. Guo, Q. Huang, S. Wang and X. Shi, *J. Mater Chem.*, **20**, 5700 (2010).
20. M. Bikshapathi, S. Mandal, G. N. Mathur, A. Sharma and N. Verma, *Ind. Eng. Chem. Res.*, **50**, 13092 (2011).
21. A. Sharma, N. Verma, A. Sharma, D. Deva and N. Sankararamakrishnan, *Chem. Eng. Sci.*, **65**, 3591 (2010).
22. R. Saraswat, N. Talreja, D. Deva, N. Sankararamakrishnan, A. Sharma and N. Verma, *Chem. Eng. J.*, **197**, 250 (2012).
23. A. Ahmad, K. Kern and K. Balasubramanian, *ChemPhysChem.*, **10**, 905 (2009).
24. G. Aragay, J. Pons and A. Merkoc, *J. Mater. Chem.*, **21**, 4326 (2011).
25. V. Kumar, N. Talreja, D. Deva, N. Sankararamakrishnan, A. Sharma and N. Verma, *Desalination*, **282**, 27 (2011).
26. N. Talreja, D. Kumar and N. Verma, *Clean-Soil, Air, Water*, **44**, 1 (2016).
27. N. Talreja, D. Kumar and N. Verma, *J. Water Process Eng.*, **3**, 34 (2014).
28. P. Khare, N. Talreja, D. Deva, A. Sharma and N. Verma, *Chem. Eng. J.*, **229**, 72 (2013).
29. R. Zhang, M. Hummelga, G. Lv and H. k. Olin, *Carbon*, **49**, 1126 (2011).
30. H. Qiao, Z. Wei, H. Yang, L. Zhu and X. Yan, *J. Nanomater*, **2009**, 795928, 5 (2009).
31. L. K. Kumawat, N. Mergu, M. Asif and V. K. Gupta, *Sens. Actuator, B*, **231**, 847 (2016).
32. H. Zhang, Q. Liu, T. Wang, Z. Yun, G. Li, J. Liu and G. Jiang, *Anal. Chim. Acta*, **770**, 140 (2013).
33. J. Abolhasani, J. Hassanzadeh and E. S. Jalali, *Int. Nano Lett.*, **4**, 65 (2014).
34. E. M. Rajeshwari, N. Chandrasekaran and A. Mukherjee, *Anal. Method*, **5**, 6211 (2013).
35. X. Wang, Y. Wei, S. Wang and L. Chen, *Colloid Surf., A: Physicochem. Eng. Aspects*, **472**, 57 (2015).
36. A. R. Ferhan, L. Guo, X. Zhou, P. Chen, S. Hong and D. M. Kim, *Anal. Chem.*, **85**, 4094 (2013).
37. H. Wei, B. Li, J. Li, S. Dong and E. Wang, *Nanotechnology*, 19(9): 095501 (2008).
38. N. Ding, Q. Cao, H. Zhao, Y. Yang, L. Zeng, Y. He, K. Xiang and G. Wang, *Sensors*, **10**, 11144 (2010).

39. T. Li, E. Wang and S. Dong, *Anal. Chem.*, **82**, 1515 (2010).
40. H. Kuang, C. Xing, C. Hao, L. Liu, L. Wang and C. Xu, *Sensors*, **13**, 4214 (2013).
41. M. Beija, C. A. M. Afonso and J. M. G. Martinho, *Chem. Soc. Rev.*, **38**, 2410 (2009).
42. A. Sahana, A. Banerjee, S. Lohar, B. Sarkar, S. K. Mukhopadhyay and D. Das, *Inorg. Chem.*, **52**, 3627 (2103).
43. N. H. Kalwar, Sirajuddin, S. T. H. Sherazi, A. R. Khaskheli, K. R. Hallam, T. B. Scott, Z. A. Tagar, S. S. Hassana and R. A. Soomro, *Appl. Catal. Gen.*, **453**, 54 (2013).
44. N. H. Kalwar, Sirajuddin, R. Z. Soomro, S. T. S. Hussain, K. R. Hallam and A. R. Khaskheli, *Int. J. Metal.*, **2014**, 1 (2014).